



<https://www.abrj.org/>

Impact Factor 2.30

Engineering Human Kidneys in the Lab: A Breakthrough in Regenerative Medicine

Author Details: Sayma Nasrin Shompa

International Islamic University Chittagong.

Computer Science and Engineering, Bangladesh, Chittagong,

Email: Saimanasrin453@Gmail.Com

<https://orcid.org/0009-0004-8637-1108>

Abstract

Chronic kidney disease (CKD) is the condition that has affected a number of people globally with limited treatment options concentrating on dialysis and organ transplantation. Stem cell biology, tissue engineering, and organoid technology have been the sources of human kidney tissue that is functional and can be used in vitro. The paper explores the advances in lab-grown human kidneys and the parts of it that are made from iPSC-derived kidney organoids, bioprinting technologies, and the problems of vascularization and maturation. The paper goes on to discuss how these changes are playing a big part in the future of regenerative nephrology and also solving the problem of organ shortage around the world. Besides, we are also addressing the ethical, technical, and translational problems that need to be solved so that lab-grown kidneys can be easily come from the bench and used at the bedside. The generation of kidney organoids and models produced by bio printing is a big step in the history of regenerative medicine. The paper addresses several topics open in the field of kidney organoid culture, neural crest and placode interactions, and 3D bioprinting technologies. In this paper we are reviewing the molecular and developmental biology of the process of organoid formation and the bioprinting innovations integrating them and providing a comprehensive Helicopter overview of kidney regeneration strategies. This merging gives the reader an insight into the whole-organ engineering, patient-specific therapies, and drug screening opportunities and challenges in the future

Keywords: *Kidney organoids, regenerative medicine, stem cells, iPSC, tissue engineering, 3D bioprinting, nephrology.*

I. Introduction

Chronic kidney disease (CKD) now stands as a pressing concern towards a person's well-being as a global health issue [1]. Currently available treatment methods such as dialysis and donor transplants do not meet the ever-growing demand. The creation of bioengineered kidneys utilizes the potential of regenerative medicine and as such is extremely critical in effectively aiding the rest of the patients. [2].

More recently, advancements in the field of cell stem reprogramming, and particularly iPSCs have permitted the creation of kidney organoids that replicate the initial phases of the kidney's development [3]. Renal tissues that possess the ability to filter, reabsorb, and generate several hormones are now being approached and as such are a result of research in bioprinting, microfluidics, and synthetic scaffolding [4].

Kidney organ and interstitial diseases are one of the leading global health concerns as they adversely affect the human population requiring kidney dialysis or organ transplantation [1]. However, the rejection issues paired with the organ deficiency problem means there should be re-evaluated regenerative medicine

strategies. Organoids are and have provided on the global stage a powerful medium for the studies on organ development, pathological phenomena and associated diseases and also for testing the various pharmacologic agents that are available [2], [3]. Encouraged with the knowledge that scientists have gotten throughout the embryonic development and with the help of the 3D bioprinting, these methods direct the construction of kidney tissues in vitro.

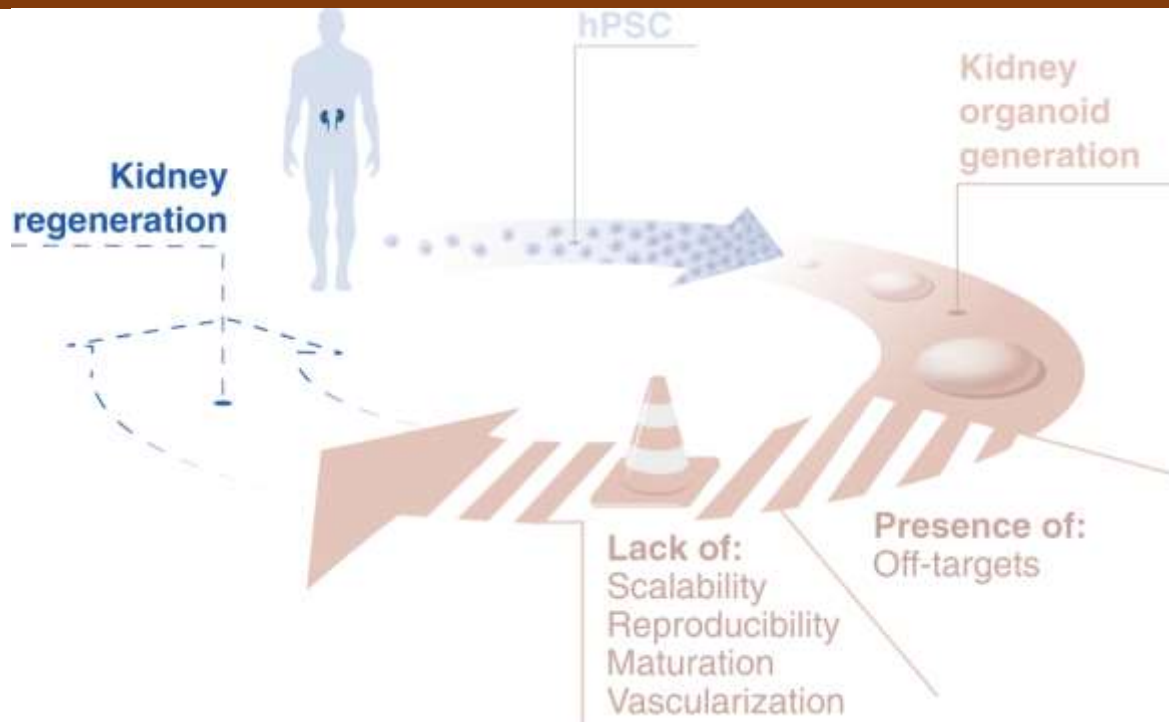
The human kidney can be characterized as a complex organ having several functions such as filtration, performing homeostasis, and executing the endocrine actions. Today these issues are addressed with dialysis and in some cases transplant surgery, however these interventions are limited in their effectiveness. With the advent of 3D bioprinting and organoid technologies, regenerative medicine is quickly advancing. There is significant work that still needs to be done in order to be clinically available such as: the construct vascularization to sustain larger tissues, proper long term functional integration, and safety regulations. Still, bioprinting and organoid science convergence have the greatest capability in the advancement of regenerative nephrology, providing hope for effective treatment in the near future. Inadequate treatment options, coupled with an increased global population, has made chronic kidney disease (CKD) one of the most crucial contemporary global issues. Partnered with chronic kidney disease is an increased need and desirability for kidney transplant surgery, making bioengineered kidneys an inviting goal of modern medicine. Improvements in stem cell treatments are resolutely changing bioengineering due to the successful results seen with iPSC stem cells. [70-72].

II. METHODOLOGY

Kidney Organoid Engineering

The development of human kidney bioprinting and organoid models in personalized regenerative medicine continues to advance rapidly because it tackles organ donor shortages and improves kidney disease treatments. The combination of stem cell biology with tissue engineering and 3D bioprinting techniques enables the creation of personalized functional kidney tissue through these technologies. Taka Sato et al. developed kidney organoids from human iPSCs which demonstrate the ability to form nephron structures through self-organization [2]. The research by Freedman et al. employed CRISPR technology to model kidney diseases which proved organoids as effective tools for studying genetic renal disorders [3]. The development of these technologies faces ongoing challenges related to vascularization and maturation [1].

Kidney organoids, obtained from pluripotent stem cells, mimic many structural and functional characteristics of human kidney. They provide a powerful platform for disease modeling, drug testing and eventually regenerative remedies. However, there are challenges in achieving complete maturity, vascularization and functional integration of these organs. Recent work has upgraded the reproducible generation of the kidney organ using 3D bioprinting technologies, allowing accurate spatial control of various cell types and external matrix components. It increases organoid uniformity, scalability and physiological relevance, making them more suitable for individual applications. Kidney organoids are short, simplified versions, which are the simplified versions of the kidney obtained from the human -induced pluripotent stem cell (hiPSCs) such as pluripotent stem cells (PSCs). These models repeat nephron structures and are valuable for disease modeling and drug screening [1] [2] protocol has been adapted for fertility and discrimination efficiency, yet organoids still lack maturity and complete vascular complexity personal regenerative drugs to a great extent. Genetic background and disease phenotypes. This personalization series facilitates the capacity for drug screening and autologous transplant, reducing the immune rejection risk. In addition, the emergence of bio -ink by combining decellularized kidney extracellular matrix with stem cells supports a more natural microelement, promotes better tissue maturity and function [3]



Picture 1: Renal replacement therapy in regenerative medicine.

Stem Cell-Derived Kidney Organoids are a promising regenerative Medicine Therapy for Patients with Chronic Kidney Disease. Before it can be applied to the clinic, significant improvement, maturity, vascularization, fertility and scaling are required on the off-target population. [1]

Developmental Biology Underpinning Kidney Formation

To understand renal development requires insight by nerve crest and placode research. The nerve crest cells contribute to peripheral nervous system and sensory structures [4], [5], while the placed cranial form sensory organs [6,8]. Using ascidians and amphioxus, evolutionary studies detect the origin of these structures, highlighting protected routes such as FGF, BMP and WNT signaling [9,24].

Genetic pathways for differentiation of the peripheral nervous system in ascidians

The peripheral nervous system (PNSS) includes sensory neurons. In the vertebral fetus, the PNSS arises from the range of the nerve plate.] In the Enamor fetus, additional mechanistic neurons called Rohon-Burd Sensitive Neurons are also made from neural plate range [8,9], on the other hand, in safelochaledes, the most basal cordate group, in which no nerve crest cells or placodes are identified, the neurulas are obtained from the abdominal fetal area. Ciona Intestinalis is a member of the unique, who are closest to the vertebrae. In this species, pels, which contain sensory neurons and differentiate at the anterior end of the larvae, are obtained from the anterior border of the nerve plate [12]. In contrast, pigment cells, which differentiate from the brain, are obtained from the acropolis range of nerve plate [13], in fact, the anterior and astrological border of the nerve plate is suggested as an underdeveloped placode and a primitive nervous crest respectively, [14-18] Neral plate's post-racial border, dorsal cord, morcellated Chitra. 1) In addition to these PNS neurons, separated from [19], the ascidian larvae have done ESN in the abdominal area of the tail. A cell lineage analysis has shown that this abdominal area is not taken from the range of nerve plate [19]

The poster logical boundary of the neural plate is motivated in a process coordinated by four signaling molecules in the 32-cell phase [20-25]. FGF9/16/20 Activates OTX and nodal in a cell pair called signaling B6.5 (supplementary fig. 1). EFNA.D signaling (Ephrin-D, in the east, named recently published as per the rule) [26] [26], GDF1/R (which GDF1/3- or orphan TGF β 2) and Damp (a bone morphogenetic protein

(BMP) -Related Ligand controls the expression negatively. OTX transcription factor and nodal signaling MSX (east MSXB) and delta (east active the expression of delta-like or delta 2) [27,28], active the expression of [27,28], on the other hand, the ventral ESN is motivated by ADMP, which is expressed in the endoderm, which is expressed in the endoderm, which is expressed in the ventral ectodermal field [13,28] Is. Although the detailed molecular system is to be clarified, ventral ESN descent cells also express MSX and Delta. [13,29] In the nerve induction of the vertebral fetus, BMP regulates nerve fate negatively, FGFS positively induces nerve fate [30–34] and nerve crest and placodes originate from an area. In protostome, including flies and anilids [37,38] Thus, in relation to the cell dynasty and signaling required for differentiation, the anterior PNS neurons in the larvae and the dorsal PNS neurons are reminiscent of the PNS neurons in the vertebral embryos, while the ventral PNS neurons are reminiscent of PNS neurons in the anacardate and protostome embracing. Given that the innovation of nerve crest cells and placodes is considered a significant phenomenon during development ranging from primitive inconceivable corsets to vertebrae [35,39], it is possible that Ciona embryo may contain both vertebrae-type and invertebrate-type neurons in the fetus. In the current study, we dissect a gene circuit involved in the discrimination of ventral sense in the Ciona fetus, and compare it with a gene circuit involved in the discrimination of the dorsal ESN to understand the development of PNS in chordates.

Results of BMP signaling in the ventral ectodermal region

Previous studies have shown that the abdominal ectodermal area of the tail is inspired by a BMP ligand, ADMP [13,22]. To determine when and where this signaling works, we used an antibody against phosphorylated SMAD1/5/8 (PSMAD1/5/8). To confirm that this antibody is immune against PSMAD1/5/8 in the Ascidian fetus, we have first stained early-lord fetuses, in which the BMP signaling is active in the ventral trunk area [40] as shown in figs, we installed strong PSMAD1/5/8 stains in the ventral trunk area. In addition, when the BMP2/4 was oversized throughout the epidermis using the ld. upstream area, the PSMAD1/5/8 staining was found in the entire epidermis (supplementary fig. 2A, C). Conversely, when Noggin, which is an opponent for BMP ligands, was oversized, Psmad1/5/8 was barely detected (supplementary image 2b, d). Thus, this antibody successfully detected PSMAD1/5/8 in the Ascidian fetus.

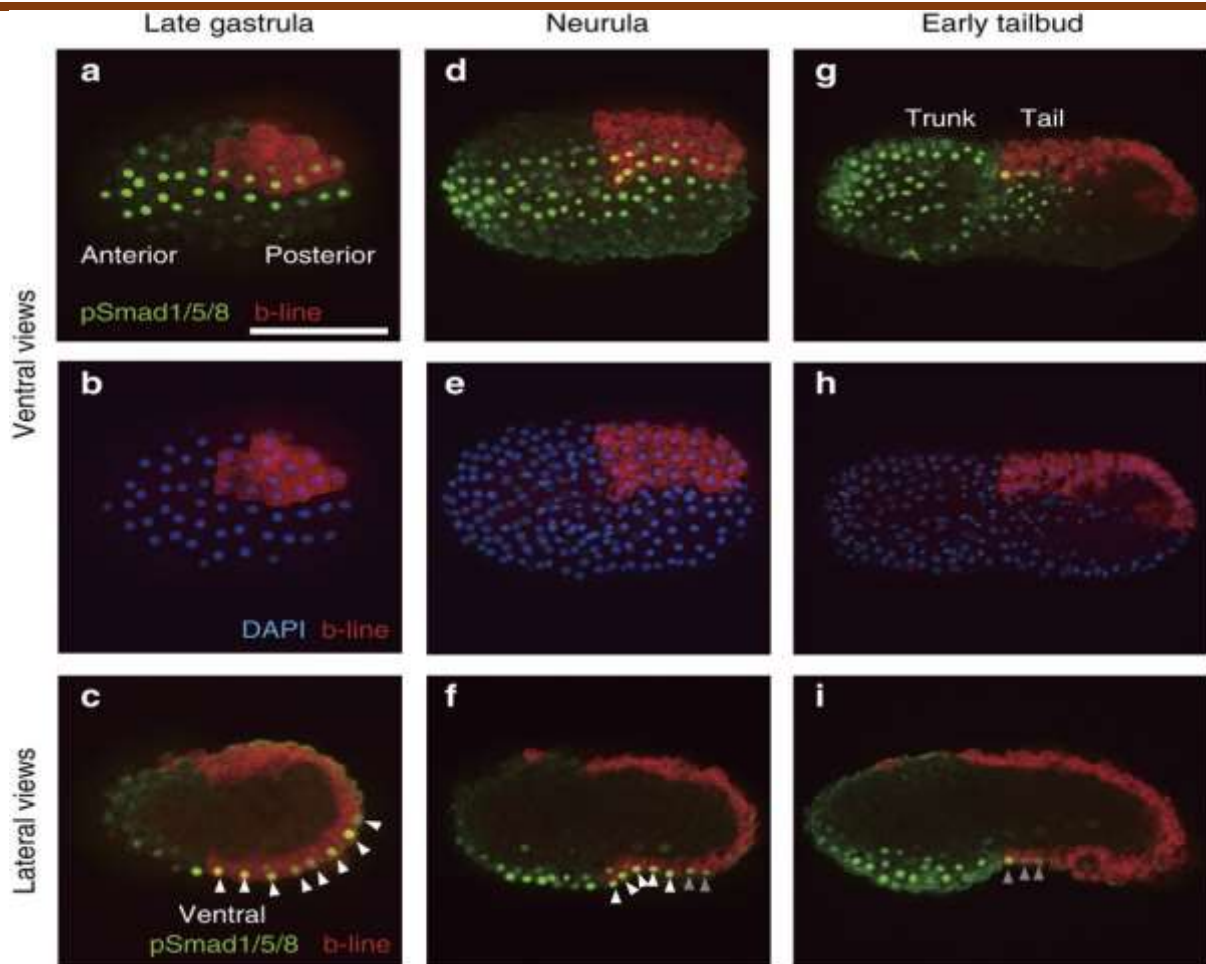


Figure 1: BMP signaling is active in the ventral ectoderm from the late-gastrula to the tailbud stages.

One of the animal cells behind the eight-cell fetus was labeled with DII (red) to show the anterior-position border and the left-right range. (B, E, H) DAPI reflects the nucleus (blue) of the fetus shown in staining A, D and G. Ventral views are shown in A, B, D, E, G and H, and lateral ideas are shown in C, F and I. Photographs are Z-proacted image stacks that are overlaid in Pseudo color. White and gray arrows in C, F and I indicate strong and weak signals respectively. Scale bar, 100 μ m (A). DAPI, 4,6-Daimidino-2-Phenylindole. [3] As shown in figs. In 1A-C, we saw staining in two rows of strong PSMAD 1/5/8 Ventral ectoderm cells in the back to the rear end in the back-gastrula phase. We labeled one of the two B4.2 blastomeres of eight-cell fetus with DII to identify the anterior range, as the tail ectoderm receives a pair of B4.2 cells. The tail region includes eight psmad1/5/8- positive rows (image 1C). The next cell division (10th division; after splitting most cells later) in the neurula phase, we detected PSMAD1/5/8 in the anterior lines within the B4.2-line ectodermal cells and in the ventral ectodermal area of the trunk (image 1D-F). B4.2-Line Ectoderm had a strong sign in five rows of the anterior, and two or three additional rows had a weak signal. After dividing the next cell division (11th division (11th division (11th division; most cells) in the early-tale bad phase, we discovered a weak psmad1/5/8 signal in only three anterior rows of B4.2-line ectodermal cells (image 1g-i).

Actually, a morpholino anticancer against PSMAD1/5/8 Storing Adm (Image 2B, D) on the late-gastrula stage was lost in the embryo injected with a morpholino antihelium oligonucleotide (Mo), while the control was not affected by the embryo, which was not affected by the embryo, which was not affected, which was with Escherichia Coli Lacs (Fig. Was injected. The BMP2/4 is activated by ADMP signaling in the ventral trunk epidermis in the tabled stage [40], and begins to be expressed in the ventral epidermis in late-Gastrula stage 26. We checked whether the expression of BMP 2/4 in the late-Gastrula phase is also inspired by ADMP, and found that BMP 2/4 expression was lost in ADMP Morphants (Image 2E, F). Because

SMAD1/5/8 can be phosphorylated and activated by BMP2/4, in addition to Adm, we collectively call BMP2/4 signaling and as BMP signaling after Adm. [3]

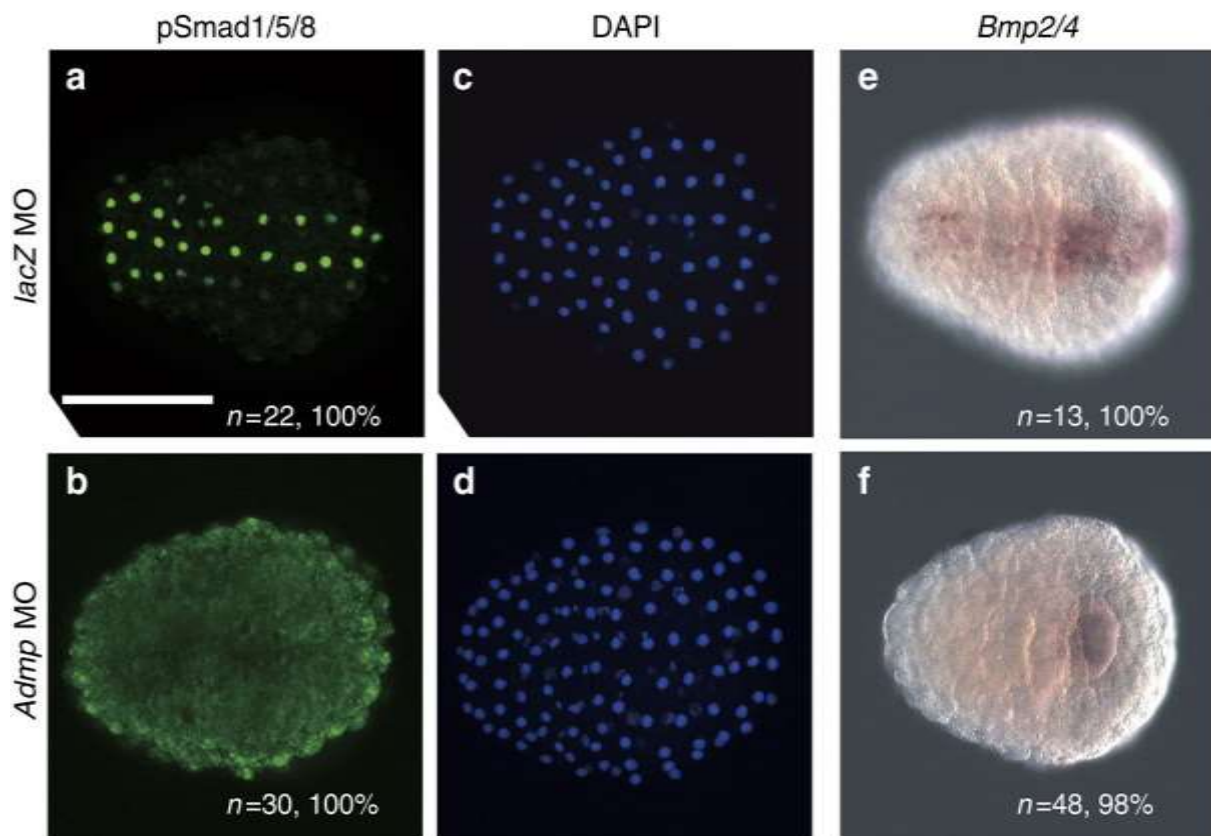


Figure 2: *Adm* activates *Bmp* signaling and *Bmp2/4* expression in the ventral ectoderm at the late-gastrula stage.

(A, B) BMP signaling was detected with antibodies against phosphorylated SMAD 1/5/8 (Hare) (A), injected with a control lase MO, and (B) an ADMP MO in an embryo. (C, D) DAPI reflects the nucleus (blue) of the fetus shown in blurred A and B., Scale bar, 100 am (A). The number of fetus and the number of fetal ratios representing each panel is shown within panels. DAPI, 4,6-Diamidino-2-Fenilindol. TBX2/3 is required for MSX expression in the ventral region

MSX is important for discrimination of the dorsal ESNs [27,28] and is also expressed in Ventral Tail Earworm [29], suggesting that MSX is also important for the discrimination of Ventral ESN. To confirm this possibility, we injected an MO in the fertilized eggs against MSX. In the resulting morphos fetus, Pou4 and Celf3.A (ETR-1), which ESNs [29,41] (see Figure 7C, E) was not marked, (supplementary image 3A, B) in the doer and ventral ESN, leaving some ESN near the tip of the tail. Because MSX has not been expressed in the back area, it is not surprising that ESNs expressed PO4 and CELF3.A near the tip of the tail of MSX Morphants. We also found that Pou4 and CELF3.A were expressed ectopically, when MSX was oversized throughout the epidermis using ld. upstream field (supplementary image 3c, D).

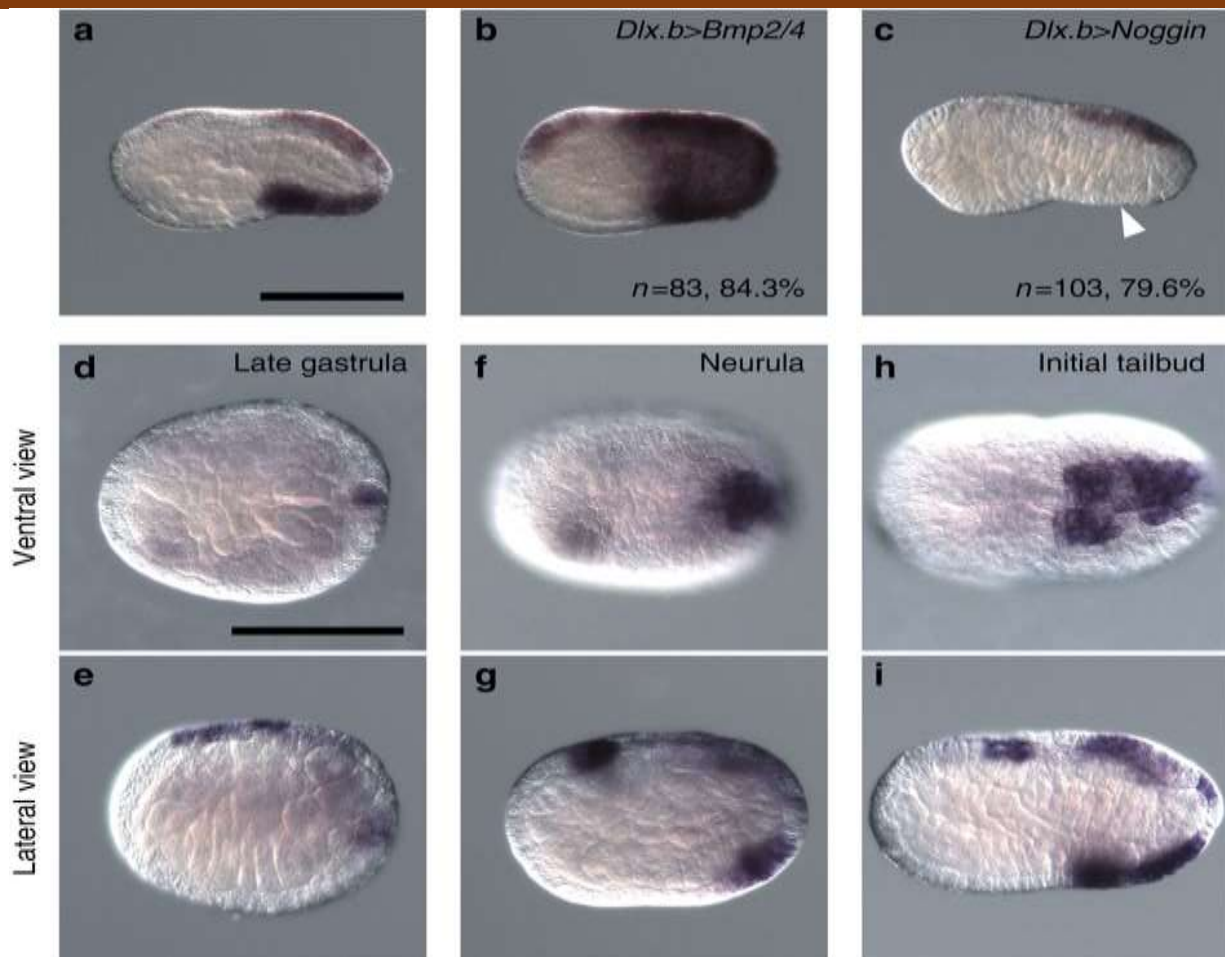


Figure 3: *Mxs* is under the control of Bmp signaling, and begins to be expressed in the ventral tail ectoderm at the neurula stage.

(A-C) MSX expression (A) In a control, an initial-tale bad fetus, (B) under DLXB enhancers with BMP 2/4 Overseas in a fetus and (C) under DLX B Ananases in a fetus with noggin overpasses in a fetus. The white arrow indicates an area in which MSX expression is lost. The number of fetus and the number of fetal ratios representing each panel is shown within panels. (D-i) MSX Expression (D, E) On Late-Gastrula Stage, (F, G) Neurula Stage and (H, I) Early-Tale bad Stage. (D, F, H) abdominal view and (E, G, I) lateral views are shown. Scale bar, 100 am (A, D). We conducted the next investigation to whether MSX began to be expressed at the same level as BMP2/4, which is active by Adm signaling, as described above. Although the expression pattern of MSX has been described earlier [29,42] We again examined the MSX expression to determine the exact time of its expression in ventral educational cells (Fig. 3D -I). The MSX was not expressed in the Ventral Ectoderm at the late-Gastrula phase, and in the neurula phase, the ventral was beginning to be expressed in half of the back of the tail eclipse. In the initial-tale bad phase, the MSX was expressed throughout the abdominal area of the tail ectoderm. Thus, because its expression begins later compared to BMP2/4, MSX Adm signaling is unlikely to be a direct target.

Candidates who are directly regulated by ADMP signaling to identify the genes and regulate MSX expression, we used RNA adaptation (RNA-CQ) to compare the gene expression in the late gastrula embryo treated with the cornier BMP 4 or BMP inhibitor, Dorsomorphin. Five transcription factor genes, including MSX, were very upgraded to the fetus treated with BMP 4 and downgrade in embryos treated with dorsomorphin (Fig. 4A). The NKXTUN1 (NKX-A) and NK2-3/5/6 (NK4) are expressed in the trunk ventral epidermis, especially in the tail stage, while the atoh8 (Net) is not expressed especially in ventral epidermis [29]. On the other hand, TBX2/3 is expressed in the abdominal ectoderm of the tail [29,43,44] so we set the exact time of initiation and expiration of TBX2/3 expression (image 4B -G). In the late-Gastrula phase, the TBX2/3 was expressed in the entire ventral ectoderm (Image 4B, C). In the neurula phase, the expression of

TBX2/3 was reduced to half of the tail ectoderm, and the rest of the ventral was weakened in ectoderm (Fig. 4D, E). In the initial-tale bad phase, the expression of TBX2/3 completely disappeared in the ventral tail eclipse (Fig. 4F, G). Thus, expression of TBX2/3 before MSX expression. The TBX2/3 was actually activated by BMP signaling, as displayed by observation that it was expressed ectopically in the BMP2/4-Overexpressing fetus (Image 4H).

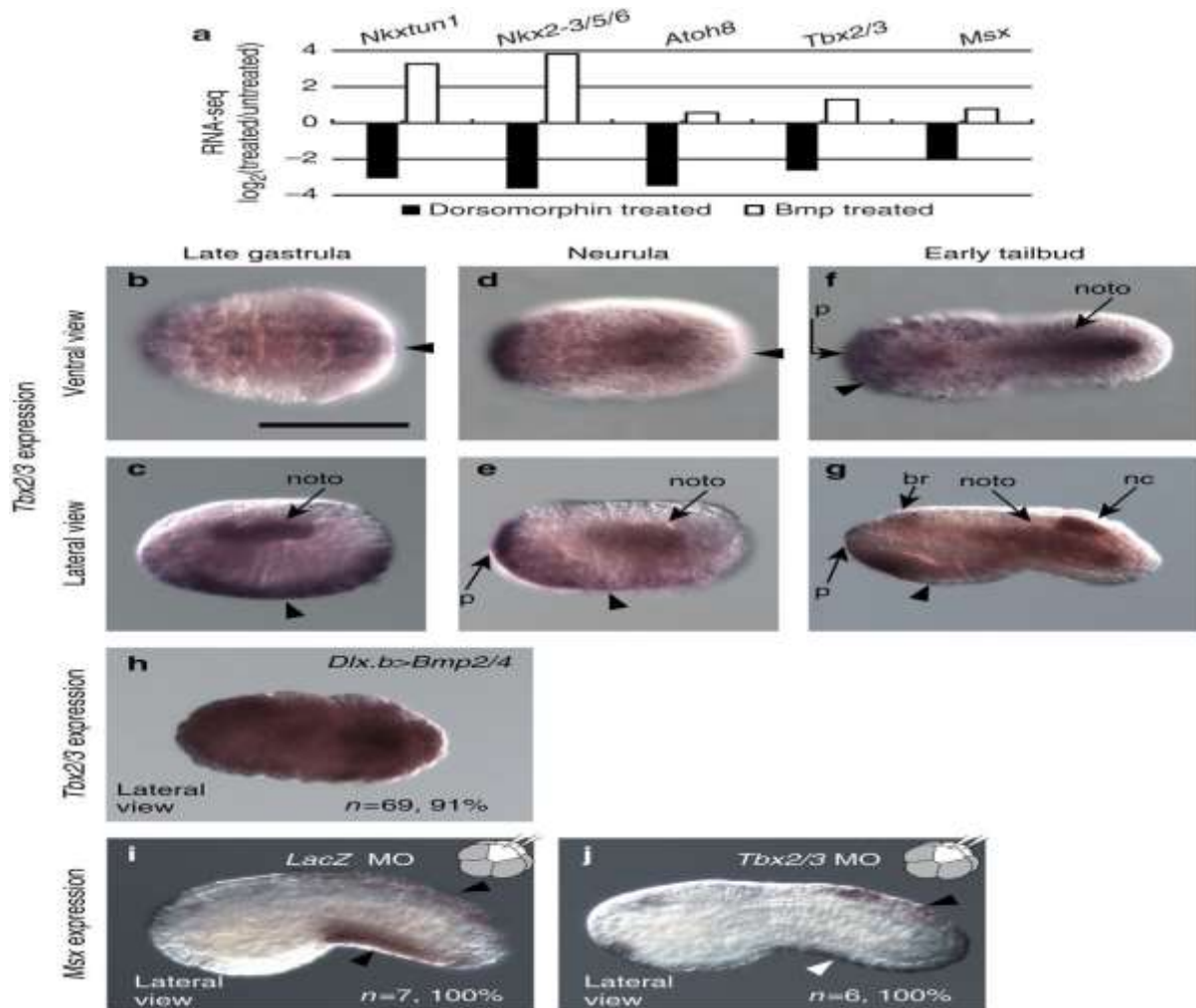


Figure 4: Tbx2/3 is expressed under Bmp signaling and regulates Mxs expression in the ventral ectoderm.

RNA-SEC experiments had upgraded and downgrade five transcription causes in fetus treated with BMP4 and dorsomorphin, (Pointed by Ponn A number of tests <0.01 , which was calculated by DESI [55]; Respectively). (B-G) TBX 2/3 expression (back) in late-gastrula phase, (fixed) neurula phase and (F, G) initial-tabled phase. The expression in Ventral Ectoderm is indicated by arrowheads. Note that the TBX2/3 is also expressed in the notecard (note), nerve cord (neck), brain (by) and polyps (p). While the MXS expression was not affected (i) TBX2/3 Morphant in the dorsal area of the fetus (black arrow) in the embryo injected with Lacs MO and (J), it was greatly reduced in the abdominal area of the TBX2/3 Morphant fetus (white arrow). Scale Bar, 100 pm (B). The number of fetus and the number of fetuses representing each panel and the ratio of fetus shown in H - J. All fetuses are shown with the anterior to the left.

Subsequently, we injected a TBX2/3 Mo in both left and right B4.2 blastomeres on the eight-cell stage that TBX2/3 should be regulated to MX in tail ectoderm cell-autonomy [29] (we have not injected Mo in the fertilized eggs, because TBX2/3 is also expressed in non-bean cells). In these TBX2/3 Morphants, the MXS expression was downed into the abdominal tail ectoderm of the tabled fetus, but the page was unaffected in ectoderm (Fig. 4i, J). For another confirmation, the TBX2/3 Mo was injected into one of the animal cells

behind the eight-cell fetus (B4.2), the MXS expression was lost in the abdominal area on the side (supplementary image 4A, B) injected. Thus, the BMP signaling activates the TBX2/3 in the ventral tail ectoderm in the late-gastrula phase, and TBX2/3 is required to activate MXS. Although MXS expression in Ventral Tail Anoderm requires TBX2/3, it may be insufficient for MXS expression. This is because the TBX 2/3 Messenger RNA (MRNA) failed to develop the ectopic expression of MXS (supplementary image 5) injected into the fertilized eggs. BMP signaling itself or unknown factor can work to activate MX, combined with TBX 2/3 of BMP signaling. SC.B. And tox tails are activated by MXS in Ectoderm Because Sc.B., Tail Ear Anoderm.

The expression of these two genes in the ventral tail ectoderm was not detected in the late-gastrula or neurula phase, and began in the tales in the normal fetus (image 5A-al). These genes were strongly expressed in the ventral tail ectoderm, except for several cells near the trunk-tell border in the initial-tale bad phase. In the initial-tale bad phase, both genes began to be expressed throughout the tail ventral ectoderm. Thus, SC.B. Expression of. And tox later began compared to MXS expression.

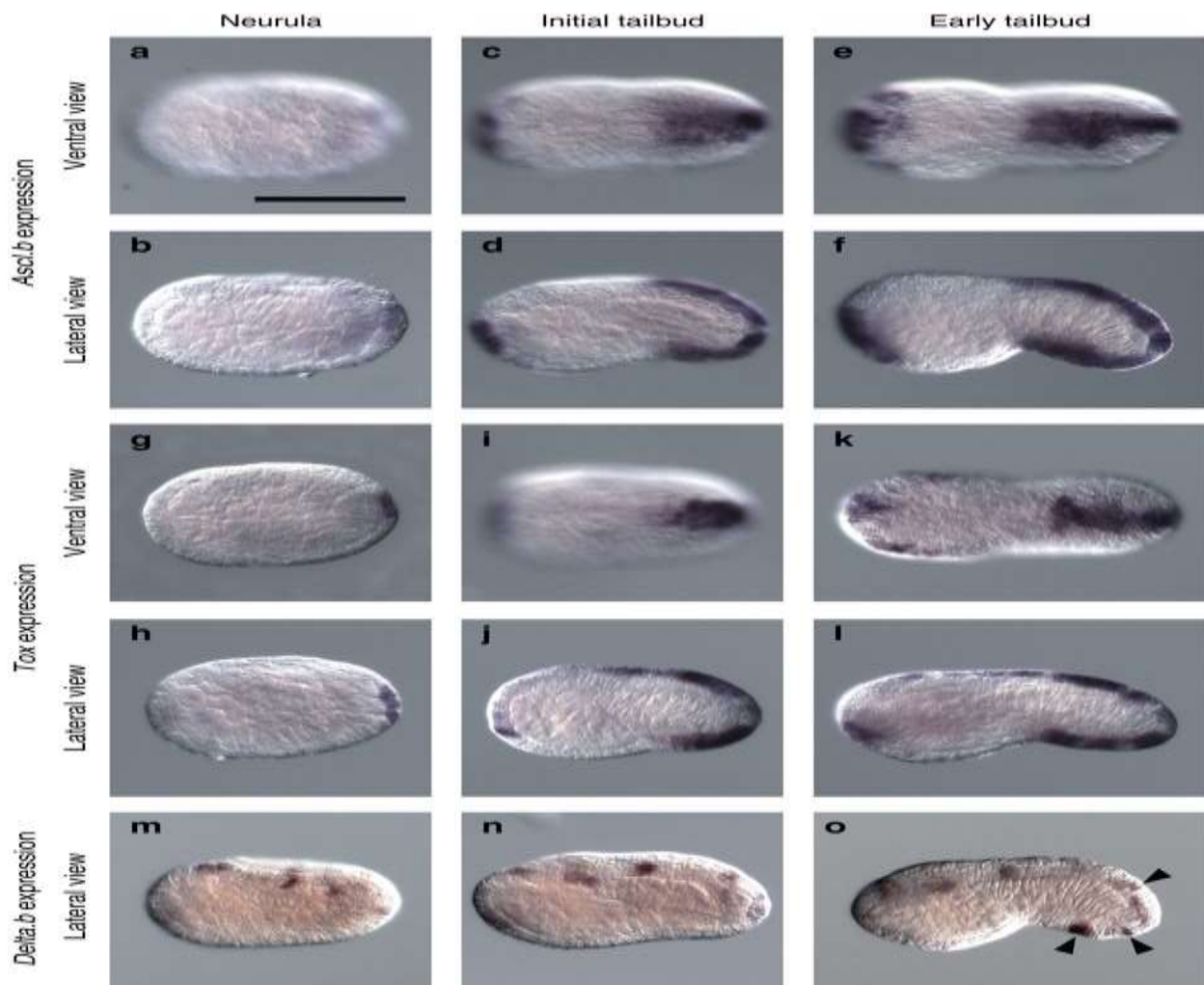


Figure 5: *Sc.B.* and *Tox* expression begins at the initial-tailbud stage and precedes *Delta*'s expression.

(A -H) (A -F) expression of SCB, (G -L) *Tox* and (M -O) *Delta*. (A, B, G, H, M) in the neurula phase, and (C, D, I, J, N) Early-Tebald Stage, and (E, F, K, L, O) Early-Tale bad Stage. (A, C, E, G, I, K) abdominal view and (B, D, F, H, J, L -O) are shown lateral views. Potential sense is indicated by black arrows in O. Scale Bar, 100 pm (A). We first confirmed that the injection of the MO did not affect the expression of SC.B. And *tox* (image 6A, b). Subsequently, we injected a Mo against TBX2/3 in both left and right B4.2 blastomeres. In the resulting occurrence fetus, expression of SC.B. And the *tox* in the tail ventral ectoderm

was greatly reduced, while the expression of two genes in the dorsal ectoderm, in which the TBX2/3 was not expressed, was not affected (Image. 6C, D). Similarly, the TBX2/3 Mo was injected into one of the animal cells behind the eight-cell fetus (B4.2); Expression of SC.B. And the tox was lost in the ventral region on the injected side (complement fig. 4C -F). In MXS Morphant, expression of SCB. And except for a few cells near the tip of the tail, the tox in the dorsal and abdominal ectoderm was also lost (image 6e, F). Thus, expression of SC.B. And in the dorsal ectoderm is under the control of the tox MXS, but the TBX is not 2/3, while the expression in Ventral Earworms is under the control of TBX 2/3 and MXS.

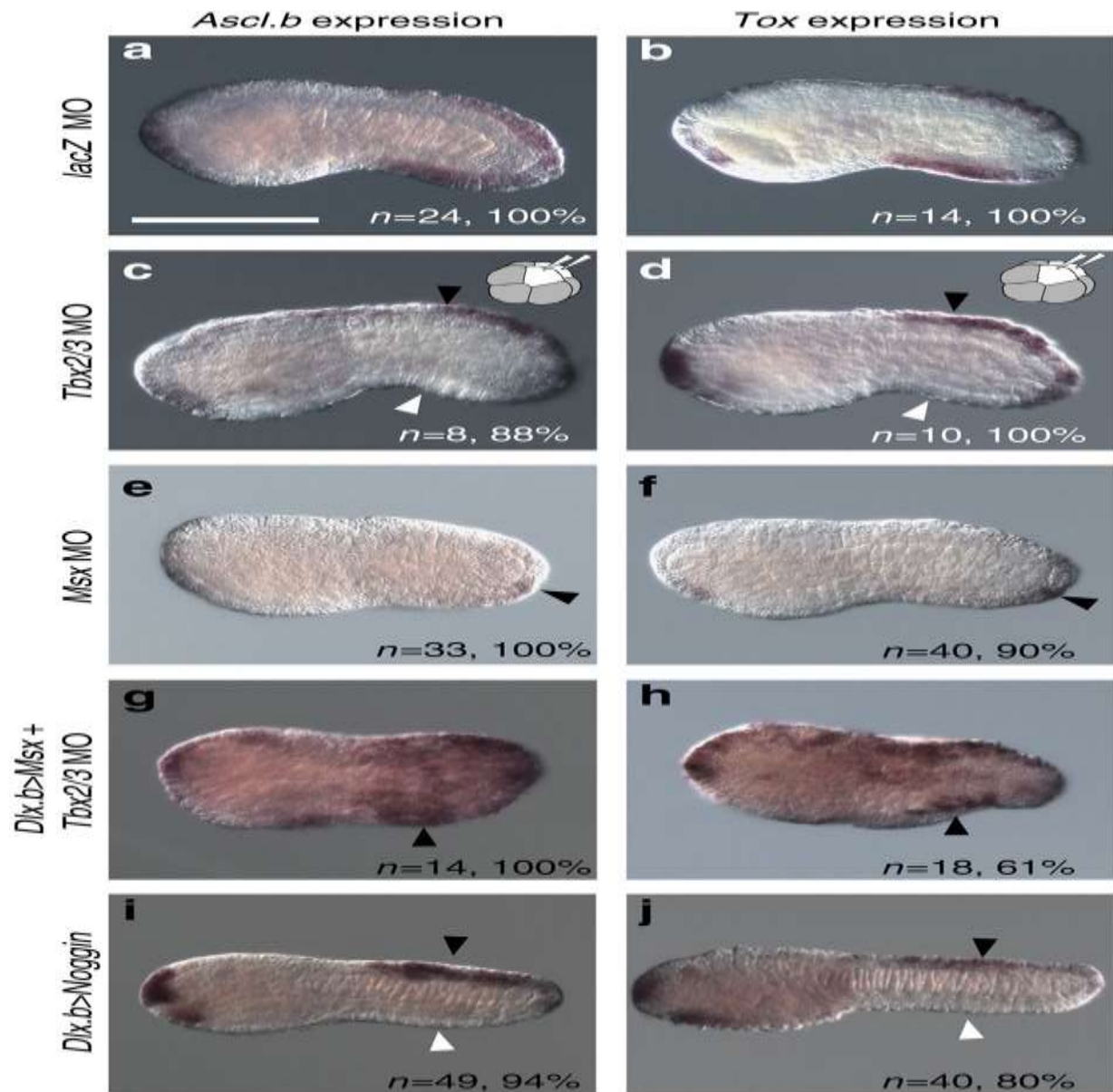


Figure 6: *Sc.B.* and *Tox* are under the control of *Tbx2/3*, *Mxs* and *Bmp* signaling.

Or (b) tox. (Cod) When the TBX2/3 Mo was injected into the left and right animal cells (B4.2) of the eight-cell fetus, (c) the expression of SC.B. And (D) Tox was very low in the ventral region (white arrow), but not in the dorsal area (black arrow). (Yogini) (E) expression Sc.B. And (f) both the tox in the ventral and dorsal regions were lost in MXS Morphants, leaving some cells in the back area (black arrow)., And (H) tox was seen in the ventral region (arrowheads) and the lateral epidermal region. With this construction, MXS was oversized throughout the epidermis under the control of LD's upstream sequence. Note that all epidermal cells do not overtax MX due to mosaic incorporation of electroporated plasmids. (i, j) expression of (I) Sc.B. And (J) the tox was lost in the ventral region (white arrow), but in the control of LD's upstream sequence,

not in the dorsal area (black arrowheads) of the fetus with noggin overaction. The number of fetus and the ratio of the fetus representing each panel is examined. Scale Bar, 100 pm (A).

We also found that the expression of SC.B. And the tox was recovered in the tail ventral ectoderm and was observed ectopically in the head and tail ectoderm, when the MXS version construction was introduced in the eggs fertilized by the Electroporation and then the TBX 2/3 MO was injected into both left and right in B4.2 Blastomeres (fig. 6G). Therefore, MXS can activate SC.B. And in the absence of TBX2/3 tox, and TBX2/3 Control SC.B. And tox through activation of MXS. Finally, we examined the expression of SC.B. And the tox in the fetus with noggin version using LD. Anansi. In these embryos, the expression in the ventral tail ectoderm was particularly lost (Fig. 6i, J). This observation confirmed that BMP signaling is required for genes active in the ventral tail ectoderm. [3]

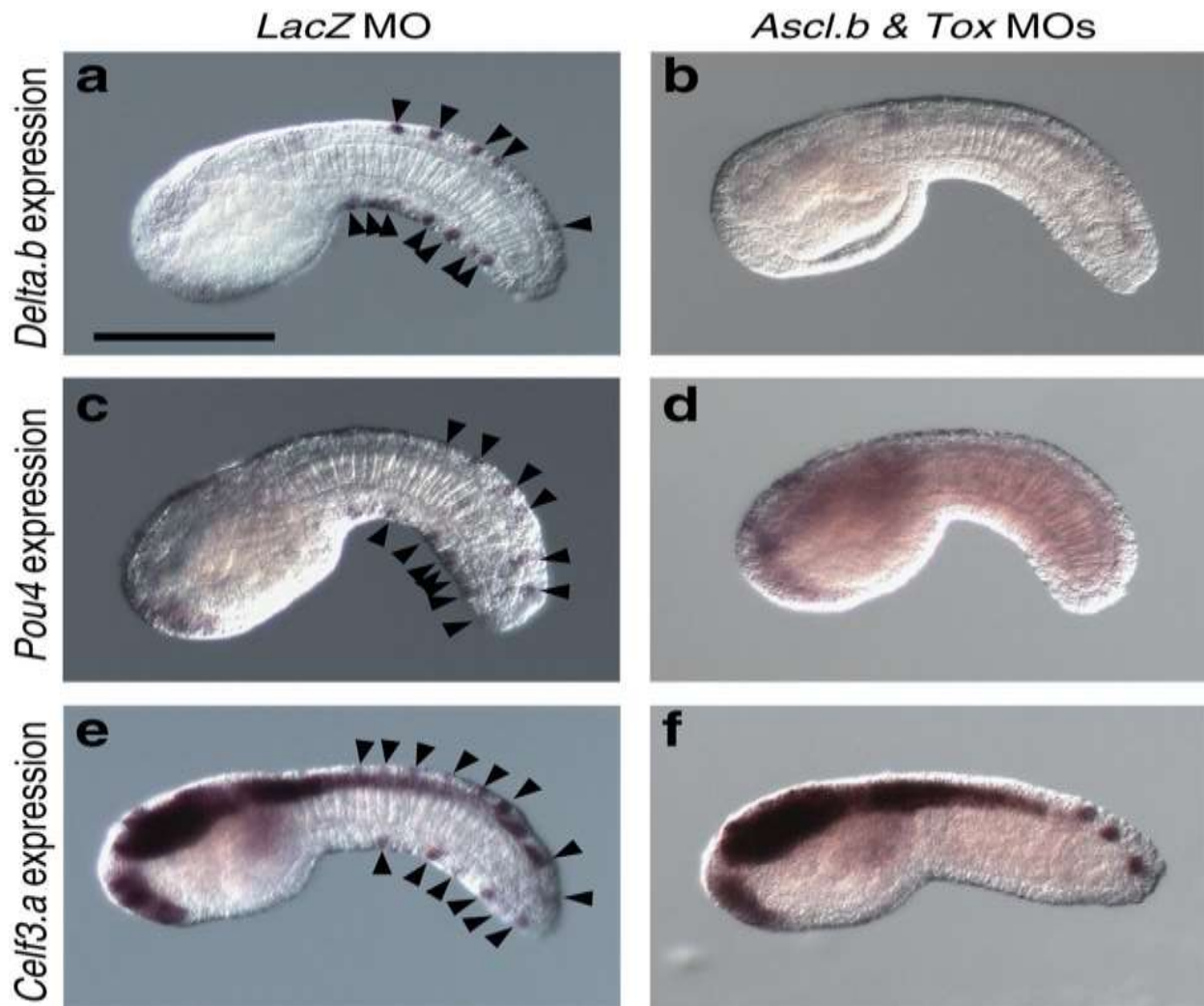


Figure 7: *Sc.B.* and *Tox* regulate *Delta*'s, *Pou4* and *Celf3.a*, which mark ESNs.

(AM) Delta, (COD) PO4 and (ELF) expression of Celf3.A, controls Sen's (Black Rehomed) (ACME) in the control fetus, which is injected with control Lacs Mo, but is completely lost in the double morpho of SC. B (b, d, f). And tox. Lateral views are shown. Note that F has the three spots nerve cord cells seen near the tip of the tail, but not ESN. A previous study has shown that the expression of CELF3.Aan in Ventral ESN is under the control of BMP signaling [19], in the current study, we found that the expression of MX in Ventral Tail Anoderm was equally downwards as BMP signaling, as MXS expression in the ventral tail ectoderm was upgraded. The embryo was downed in the fetus with engrained, and noggin (image 3A -C).

***Tox* and *Sc.B.* are required for differentiation of ESNs**

The delta is expressed in the dorsal and abdominal sense, and the signaling of the delta presses the Pou4 and Celf3.A (ETR-1) in the surrounding epidermal cells [19,27,45]. The expression of the delta in the ventral tail ectoderm begins in the scattered cells of the rear region and later in the anterior tail region [19] the delta/not -mediation spreads through the lateral prohibition, the number of neurons is controlled [19] We first examined whether there is a expression of SC.B. And the tox did before expression of delta in dorsal and abdominal ESN. The delta was not expressed in the potential ESN in neurula and early-tale bad stages (Fig. 5m, N), and began to be expressed in the potential ESN in the initial-tabled phase in the rear region (Image 5O). At the stage of the middle-tail, the potential ESN in the anterior tail region began to express [19] of the delta (see Figure 7A too). Thus, the expression of delta in potential ESN took place one step after the initiation of SC.B. And tox expression.

When we injected Mos against SC.B. Or the expression of tox, delta, pou4 and celf3.A is lost or reduced to most embryos (Table 1; Supplementary Figure 6). In SC. B's double orient. And tox, the expression of these three genes was almost completely lost (Table 1; Fig. 7A -F). Thus, SC.B. And both tox are essential for discrimination of sense in ventral and dorsal ectoderm.

Marker genes examined	Morpholinos	Embryos expressing designated marker prospective ESNs	not the Embryos expressing designated marker in prospective ESNs	Embryos expressing the designated marker in one reduced number of prospective ESNs*	the Embryos expressing the designated marker as in wild-type embryos*
<i>Delta's</i>	<i>LacZ</i>	0	0	0	8 (100%)
	<i>Sc.B.</i>	20 (57%)	13 (37%)	0	2 (6%)
	<i>Tox</i>	24 (29%)	20 (25%)	30 (37%)	7 (9%)
	<i>Sc.B. and Tox</i>	27 (100%)	0	0	0
<i>Pou4</i>	<i>LacZ</i>	0	0	1 (9%)	11 (91%)
	<i>Sc.B.</i>	33 (91%)	1 (3%)	2 (6%)	0
	<i>Tox</i>	8 (32%)	2 (8%)	13 (52%)	2 (8%)
	<i>Sc.B. and Tox</i>	26 (86%)	2 (7%)	0	2 (7%)
<i>Celf3.a</i>	<i>LacZ</i>	0	0	0	12 (100%)
	<i>Sc.B.</i>	24 (83%)	4 (14%)	1 (3%)	0
	<i>Tox</i>	21 (44%)	15 (31%)	12 (25%)	0
	<i>Sc.B. and Tox</i>	26 (90%)	2 (7%)	0	1 (3%)

Table 1: Effects of knockdown of *Sc.B.* and *Tox.*

1. ESN, epidermal sensory neuron.
2. Because the number of ESN varies between individuals [46], we counted the number of potential ESN expressing PO4 in 63 unexpected embryos. Because the minimum number of potential ESNs was seven, fetus with two to six cells was considered as a low number of ESN expressing any markers, while embryos with seven or more cells were expressed either marker.

III. Discussion

A previous study stated that there are two morphological populations between the ESN of the Ventral Tail Anoderm, as the rear ESN has a longer axon compared to the anterior ESN [46] Our analysis has shown that the ventral tail uses a single gene circuit with BMP in the anterior and rear parts of the tales, and using a single gene circuit with BMP, and using Maxi time using Maxi time. Is., we showed that TBX2/3 is required for MXS expression in Ventral Ectoderm. Although TBX2/3 and its orthologues, TBX2 and TBX3, often serve as a repressor, TBX2 and TBX3 are also known to act as workers [47,48] Therefore, it is not surprising that TBX2/3 is not surprised that the TBX2/3 directly activates MX in the ventral ectoderm.

We also showed that ventral and dorsal tail sense are specified by a common genetic passage, including MXS, Tox/SC.B. And Delta/Celf3.A/Pou4, while the upstream mechanism of MXS regulation varies between these two genealogies (Fig. 8). In the dorsal dynasty, MXS expression [27,28] requires *otx* and *nodal*, and these two genes are activated by combining the active effects of FGF signaling and combining the oppressive effects of Ephrin, ADM and GDF1/3-R signaling. TBX2/3 expression is essential for MXS expression. Therefore, evidence of co-co-disgrace of MXS's Down stream's gene circuit has created a novel dynasty of ESNS. If yes, which dynasty represents the original one? We favor the hypothesis that the abdominal dynasty is one, for two reasons. First, the ventral dynasty is inspired by BMP signaling, and PNS neurons in the amphioxus and protostome are also inspired by BMP signaling [36-38], although the cells that originate dorsal ESN in ascidian fetus are embedded in the epidermis, which are not in the Dorel dynasty, the position of the Dorel dynasty, the status of the Kasher PNSSS She does.

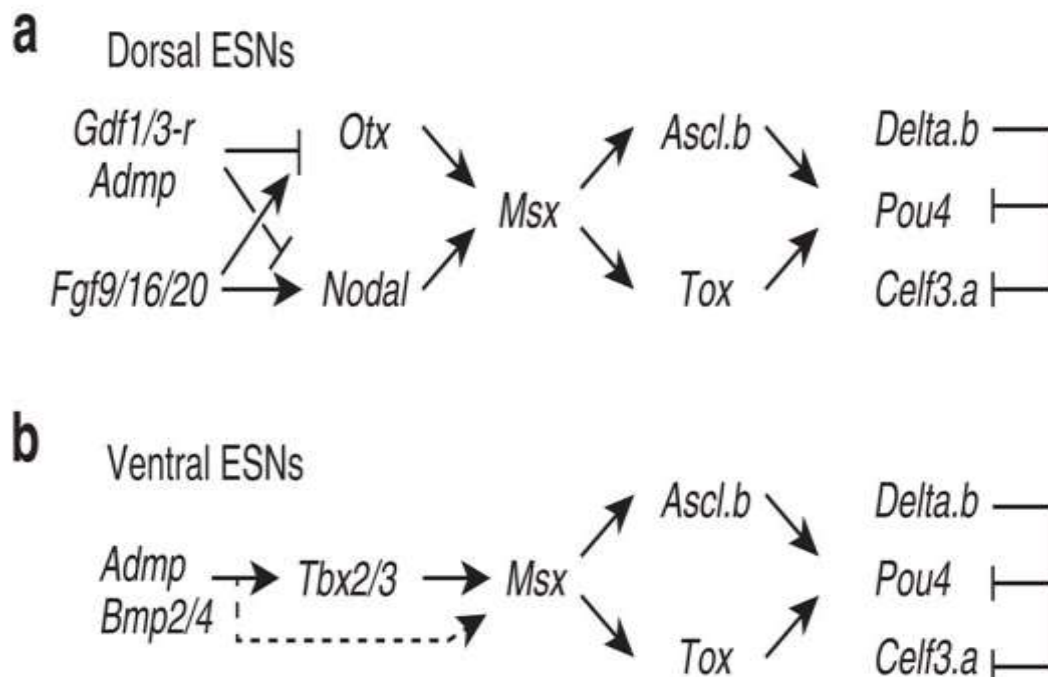


Figure 8: Summary of the regulatory gene circuits involved in differentiation of the dorsal and ventral ESNs.

(A) dorsal ESN and (B) Share a gene circuit of ventral ESN MX downwards, while the regulatory mechanisms of MX's upstream vary between these two lineages. These circuits are based on the results of current and previous studies [19,27,28,46]. Because TBX2/3 failed to activate MXS alone, BMP itself can work to activate MXS (a dotted arrow) with unknown factor, tBX2/3 at the bottom of BMP signaling. In the anamniote embryo, Rohon-bird mechanistic neurons are also made up of nerve plate range [8]. A physical study suggested that Rentzias bipolar cells of Amphioxus are similar to Rohon-Burd Sensory Neurons [49]. It is possible that Ascidian dorsal ESNs are homogeneous for Rohon-bird neurons, and this possibility is not necessarily unique with the above possibility that the Ascidian dorsal ESN is symmetrical for vertebrae PNS neurons derived from nerve peak cells. In fact, the gene network specifying Rohon-Burd Neurons and nerve crest is largely overlap [50] None of this scenario is inconsistent with our hypothesis that a novel dynasty of ESN was born from the co-co-conduction of the gene circuit under MX.

In the vertebral fetus, BMP signaling controls nerve fate during the initial process of nerve induction, but later an intermediate level of

BMP signaling is required for nerve crest formation [51,52]. MXS is actually a direct target of BMP signaling on the neural plate range [53]. However, because MXS ascidian fetal ventral ectoderm may not have a direct target of BMP signaling, the gene circuit that includes BMP signaling, TBX 2/3 and MXS in the ascidian fetus, not directly relevant with the gene circuit that activates the MXS in the Kashrut fetus. Available, available data that shows that a general ancestor of Ciona and vertebrae acquired the secondary PNS dynasty around the nerve plate range by co-disagree of the gene circuit active by MXS. Thus, the abdominal sense of the ascidian larvae may not be directly symmetrical for vertebrae pens, and the original lineage may be lost in the vertebrae.

IV. 3D Bioprinting Technologies

Kidney ancestor cells and three dimensions vary from bioprinting technology to collect biomaterials, including extrusion-based methods and microfluidics. These methods have demonstrated the ability to produce tissue -like tissue with nephron structures and support cell feasibility and discrimination. For example, extrusion bioprinting has been used to automatically to create the formation of self-organoids of kidney organoids, which further enhances the ability of scalable manufacture of patient-specific tissue constructions. The 3D bioprinting enables a layer-by-layer statement of bio ink, including cells and external matrix (ECM) content. Major bioprinter for the manufacture of kidney include -cricketers:

- I. Extrusion-based printing [55,56]
- II. Inkjet Biopriming [57]
- III. Microfluidics and light-assisted bioprinting [58]

These technologies allow the exact spatial location of various kidney cell types to mimic the native architecture of the kidney. Bioprinting provides the architectural and cellular precision required for organ construction. Technologies such as Inkjet and Extrusion Bioprinting allow the spatial placement of many cell types [59], [63]. Jung et al. The ECM used to print complex tissue structures, while the skylarks et al. Vascular network integration [64], [66] performed. Kidney-specific applications include bio printed proximal tubule models for filtration studies [65] and IPSC-derived patient-specific organoids [62] for individual medications.

3D Bioprinting and Scaffold Design

Using 3D bioprinting, bio-shaped material is layered with spatial precision to mimic kidney architecture [75]. Researchers are integrated into scaffold to endothelial cells to encourage vascularization, an essential component for oxygen and nutrient exchange [76].

V. Personalized Medicine Applications

Personal regenerative drugs greatly benefit from these developments, as patient-individuals can be used to produce renal organoids or bioprinter constructions that can be used to produce individual genetic backgrounds and disease phenotypes. This personalization series facilitates the capacity for drug screening and autologous transplant, reducing the immune rejection risk. In addition, the emergence of bio ink with a combination of decellularized kidney extracellular matrix with stem cells supports a more natural microelement, promotes better tissue maturity and function [59] The combination of bioprinting with patient-related iPSCs supports the development of autologous kidney tissue that matches the patient's genetic profile. This approach is highly beneficial for drug testing, especially in nephrotoxicity assessment [8], and paves the way for individual transplant treatments [60].

VI. Bioinks and Extracellular Matrix Composition

Natural and synthetic bio ink has been discovered to support kidney-specific tissue development. Hydrogel cells made of aligned, gelatin, collagen and ECM from decidualized kidney tissue increase viability and discrimination [61] [62].

VII. Challenges and Future Directions

Large obstacles include:

- I. Vascularization: The inclusion of endothelial network is required to maintain functional tissue size [63] [64].
- II. Functional Integration: Engineer Kidney Ensuring is integrated with host tissue on implants [65].
- III. . Regulators and moral concerns: approval routes for bio -printed organs are uncertain [66].

The ongoing research is aimed at solving these issues using advanced microfluidics, AI-directed scaffold design and gene editing technologies such as CRISPR-CAS9. Major obstacles include achieving complete organ functionality, scaling organoid production

and ensuring immune compatibility. The combination of stem cell biology, bio -engineering, and developmental genetics is important [67], [68]. As this IPSC-derived kidney organoids Protocol developed by Taka Sato et al. [2] and Freedman et al. [3] Allow for discrimination of iPSCs in structures like nephron. These organoids typically include podocytes, proximal ducts and glomeruli, but lack of vascular integration on a full scale. Microfluidics and sprayed bioreactor Recent efforts include aromatic organoid cultures using microfluidic chips. These systems repeat shrinking stress and mechanical signs in vivo conditions [77], promoting maturity and functional discrimination.

VIII. RESULTS AND DISCUSSION

Recent studies display the ability of renal organ to model nephrotoxicity [78], genetic disorders [79], and proteinuria [80]. Some partial urine such as fluid production also show [81]. However, scalability, maturity and immune compatibility challenges remain. Vascularization has seen progress through transplantation in the mouse model, where hosts are integrated into the blood vessels oroides [82]. Ethical concerns also persist, especially about the chimeric model and long -term integration in humans [83].

IX. FUTURE PROSPECTS

Integration of CRISPR gene-editing, patient-specific iPSCs, and vascular grafting technologies can enable individual kidney regeneration [84]. In addition, engineer can increase the traceability of tissues for blockchain-based patient data system transplant [85].

X. Conclusion

Bio -printed human kidney tissue and organoid models represent a transformative leap in regenerative nephrology. With further purification, these technologies promise not only for transplant, but also to develop personal medical intervention for kidney diseases. The convergence of organoid research, bioprinting and developmental biology indicates a transformative phase in regenerative medicine. Continuous innovation and cross-disciplinary collaboration will be important in translating these advances in clinical applications from the lab. The creation of human kidney developed in the laboratory represents a paradigm change in regenerative medicine. While complete transplantation--organs remain the future goals, the current progression shows immense ability in modeling, drug testing and partial therapeutic support. Continuous interdisciplinary cooperation will be important to overcome the current boundaries.

XI. Acknowledgement

I just want to take a moment to say thanks to the Computer Science and Engineering Department at the International Islamic University Chittagong. Their help and resources really made a difference in this research.

XII. References

- 1) Geuens, T. et al. (2020). Overcoming kidney organoid challenges for regenerative medicine. *npj Regen Med.* <https://www.nature.com/articles/s41536-020-0093-4>
- 2) Taka Sato, M. et al. (2015). Kidney organoids from human iPS cells. *Nature.* <https://www.nature.com/articles/nature15695>
- 3) Freedman, B. et al. (2015). Modelling kidney disease with CRISPR-mutant kidney organoids. *Nature Communications.* <https://www.nature.com/articles/ncomms9719>
- 4) Steventon, B., Mayor, R. & Streit, A. Neural crest and placode interaction during the development of the cranial sensory system. *Dev. Biol.* **389**, 28–38 (2014). <https://doi.org/10.1016/j.ydbio.2014.01.021>
- 5) Baker, C. V. & Bronner-Fraser, M. Vertebrate cranial placodes I. Embryonic induction. *Dev. Biol.* **232**, 1–61 (2001). <https://doi.org/10.1006/dbio.2001.0156>
- 6) Graham, A. & Begbie, J. Neurogenic placodes: a common front. *Trends Neurosis.* **23**, 313–316 (2000). [https://www.cell.com/trends/neurosciences/issue?pii=S0166-2236\(00\)X0061-6](https://www.cell.com/trends/neurosciences/issue?pii=S0166-2236(00)X0061-6)
- 7) Schlosser, G. Induction and specification of cranial placodes. *Dev. Biol.* **294**, 303–351 (2006). <https://doi.org/10.1016/j.ydbio.2006.03.009>
- 8) Lamborghini, J. E. Rohon-beard cells and other large neurons in *Xenopus* embryos originate during gastrulation. *J. Comp. Neurol.* **189**, 323–333 (1980). <https://onlinelibrary.wiley.com/toc/10969861/1980/189/2>
- 9) Meulemans, D. & Bronner-Fraser, M. Gene-regulatory interactions in neural crest evolution and development. *Dev. Cell* **7**, 291–299 (2004). [https://www.cell.com/developmental-cell/issue?pii=S1534-5807\(00\)X0041-X](https://www.cell.com/developmental-cell/issue?pii=S1534-5807(00)X0041-X)
- 10) Holland, N. D. & Yu, J. K. Epidermal receptor development and sensory pathways in vitally stained amphioxus (*Branchiostoma floridae*). *Acta Zool.* **83**, 309–319 (2002). <https://onlinelibrary.wiley.com/toc/14636395/2002/83/4>
- 11) Lacalli, T. C. & Hou, S. F. A reexamination of the epithelial sensory cells of amphioxus (*Branchiostoma*). *Acta Zool.* **80**, 125–134 (1999). <https://onlinelibrary.wiley.com/toc/14636395/1999/80/2>

- 12) Nicol, D. & Meinertzhagen, I. A. Development of the central nervous system of the larva of the ascidian, *Ciona intestinalis* L. II. Neural plate morphogenesis and cell lineages during neurulation. *Dev. Biol.* **130**, 737–766 (1988). [https://doi.org/10.1016/0012-1606\(88\)90364-8](https://doi.org/10.1016/0012-1606(88)90364-8)
- 13) Nishida, H. Cell lineage analysis in ascidian embryos by intracellular injection of a tracer enzyme. III. Up to the tissue restricted stage. *Dev. Biol.* **121**, 526–541 (1987). [https://doi.org/10.1016/0012-1606\(87\)90188-6](https://doi.org/10.1016/0012-1606(87)90188-6)
- 14) Abitua, P. B., Wagner, E., Navarrete, I. A. & Levine, M. Identification of a rudimentary neural crest in a non-vertebrate chordate. *Nature* **492**, 104–107 (2012). <https://www.nature.com/articles/nature11589#citeas>
- 15) Wagner, E. & Levine, M. FGF signaling establishes the anterior border of the *Ciona* neural tube. *Development* **139**, 2351–2359 (2012). <https://doi.org/10.1242/dev.078485>
- 16) Manni, L., Caicci, F., Gasparini, F., Zaniolo, G. & Burighel, P. Hair cells in ascidians and the evolution of lateral line placodes. *Evol. Dev.* **6**, 379–381 (2004). [Article](#) [PubMed](#) [Google Scholar](#)
- 17) Mazet, F. et al. Molecular evidence from *Ciona intestinalis* for the evolutionary origin of vertebrate sensory placodes. *Dev. Biol.* **282**, 494–508 (2005). [Article](#) [CAS](#) [PubMed](#) [Google Scholar](#)
- 18) Ikeda, T., Matsuoka, T. & Satou, Y. A time delay gene circuit is required for palp formation in the ascidian embryo. *Development* **140**, 4703–4708 (2013). [Article](#) [CAS](#) [PubMed](#) [Google Scholar](#)
- 19) Pasini, A. et al. Formation of the ascidian epidermal sensory neurons: insights into the origin of the chordate peripheral nervous system. *PLoS Biol.* **4**, e225 (2006) [Article](#) [PubMed](#) [PubMed Central](#) [Google Scholar](#)
- 20) Hudson, C. & Lemaire, P. Induction of anterior neural fates in the ascidian *Ciona intestinalis*. *Mech. Dev.* **100**, 189–203 (2001). [Article](#) [CAS](#) [PubMed](#) [Google Scholar](#)
- 21) Tassy, O., Daian, F., Hudson, C., Bertrand, V. & Lemaire, P. A quantitative approach to the study of cell shapes and interactions during early chordate embryogenesis. *Curr. Biol.* **16**, 345–358 (2006). [Article](#) [CAS](#) [PubMed](#) [Google Scholar](#)
- 22) Bertrand, V., Hudson, C., Caillol, D., Popovici, C. & Lemaire, P. Neural tissue in ascidian embryos is induced by FGF9/16/20, acting via a combination of maternal GATA and Ets transcription factors. *Cell* **115**, 615–627 (2003). [Article](#) [CAS](#) [PubMed](#) [Google Scholar](#)
- 23) Khoueiry, P. et al. A cis-regulatory signature in ascidians and flies, independent of transcription factor binding sites. *Curr. Biol.* **20**, 792–802 (2010). [Article](#) [CAS](#) [PubMed](#) [Google Scholar](#)
- 24) Hudson, C., Darras, S., Caillol, D., Yasuo, H. & Lemaire, P. A conserved role for the MEK signalling pathway in neural tissue specification and posteriorisation in the invertebrate chordate, the ascidian *Ciona intestinalis*. *Development* **130**, 147–159 (2003). [Article](#) [CAS](#) [PubMed](#) [Google Scholar](#)
- 25) Ohta, N. & Satou, Y. Multiple Signaling Pathways Coordinate to Induce a Threshold Response in a Chordate Embryo. *PLoS Genet.* **9**, e1003818 (2013). [Article](#) [PubMed](#) [PubMed Central](#) [Google Scholar](#)
- 26) Stolfi, A. et al. Guidelines for the nomenclature of genetic elements in tunicate genomes. *Genesis.* **53**, 1–14 (2015). [Article](#) [PubMed](#) [Google Scholar](#)
- 27) Roure, A., Lemaire, P. & Darras, S. An otx/nodal regulatory signature for posterior neural development in ascidians. *PLoS Genet.* **10**, e1004548 (2014). [Article](#) [PubMed](#) [PubMed Central](#) [Google Scholar](#)
- 28) Imai, K. S., Levine, M., Satoh, N. & Satou, Y. Regulatory blueprint for a chordate embryo. *Science* **312**, 1183–1187 (2006). [Article](#) [ADS](#) [CAS](#) [PubMed](#) [Google Scholar](#)
- 29) Imai, K. S., Hino, K., Yagi, K., Satoh, N. & Satou, Y. Gene expression profiles of transcription factors and signaling molecules in the ascidian embryo: towards a comprehensive understanding of gene networks. *Development* **131**, 4047–4058 (2004). [Article](#) [CAS](#) [PubMed](#) [Google Scholar](#)
- 30) Munoz-Sanjuan, I. & Brivanlou, A. H. Neural induction, the default model and embryonic stem cells. *Nat. Rev. Neurosci.* **3**, 271–280 (2002) [Article](#) [CAS](#) [PubMed](#) [Google Scholar](#)
- 31) Streit, A., Berliner, A. J., Papanayotou, C., Sirulnik, A. & Stern, C. D. Initiation of neural induction by FGF signalling before gastrulation. *Nature* **406**, 74–78 (2000). [Article](#) [ADS](#) [CAS](#) [PubMed](#) [Google Scholar](#)

- 32) Wilson, S. I., Graziano, E., Harland, R., Jessell, T. M. & Edlund, T. An early requirement for FGF signalling in the acquisition of neural cell fate in the chick embryo. *Curr. Biol.* **10**, 421–429 (2000).[Article](#) [CAS](#) [PubMed](#) [Google Scholar](#)
- 33) Marchal, L., Luxardi, G., Thome, V. & Kodjabachian, L. BMP inhibition initiates neural induction via FGF signaling and Zic genes. *Proc. Natl Acad. Sci. USA* **106**, 17437–17442 (2009).[Article](#) [ADS](#) [CAS](#) [PubMed](#) [PubMed Central](#) [Google Scholar](#)
- 34) Delaune, E., Lemaire, P. & Kodjabachian, L. Neural induction in *Xenopus* requires early FGF signalling in addition to BMP inhibition. *Development* **132**, 299–310 (2005).[Article](#) [CAS](#) [PubMed](#) [Google Scholar](#)
- 35) Bronner, M. E. & LeDouarin, N. M. Development and evolution of the neural crest: an overview. *Dev. Biol.* **366**, 2–9 (2012).[Article](#) [CAS](#) [PubMed](#) [PubMed Central](#) [Google Scholar](#)
- 36) Lu, T. M., Luo, Y. J. & Yu, J. K. BMP and Delta/Notch signaling control the development of amphioxus epidermal sensory neurons: insights into the evolution of the peripheral sensory system. *Development* **139**, 2020–2030 (2012).[Article](#) [CAS](#) [PubMed](#) [Google Scholar](#)
- 37) Denes, A. S. et al. Molecular architecture of annelid nerve cord supports common origin of nervous system centralization in bilateria. *Cell* **129**, 277–288 (2007).[Article](#) [CAS](#) [PubMed](#) [Google Scholar](#)
- 38) Rusten, T. E., Cantera, R., Kafatos, F. C. & Barrio, R. The role of TGF beta signaling in the formation of the dorsal nervous system is conserved between *Drosophila* and chordates. *Development* **129**, 3575–3584 (2002).[CAS](#) [PubMed](#) [Google Scholar](#)
- 39) Patthey, C., Schlosser, G. & Shimeld, S. M. The evolutionary history of vertebrate cranial placodes-I: cell type evolution. *Dev. Biol.* **389**, 82–97 (2014).[Article](#) [CAS](#) [PubMed](#) [Google Scholar](#)
- 40) Imai, K. S., Daido, Y., Kusakabe, T. G. & Satou, Y. Cis-acting transcriptional repression establishes a sharp boundary in chordate embryos. *Science* **337**, 964–967 (2012).[Article](#) [ADS](#) [CAS](#) [PubMed](#) [Google Scholar](#)
- 41) Yagi, K. & Makabe, K. W. Isolation of an early neural marker gene abundantly expressed in the nervous system of the ascidian, *Halocynthia roretzi*. *Dev. Genes Evol.* **211**, 49–53 (2001).[Article](#) [CAS](#) [PubMed](#) [Google Scholar](#)
- 42) Aniello, F. et al. Identification and developmental expression of *Ci-msxb*: a novel homologue of *Drosophila* *msh* gene in *Ciona intestinalis*. *Mech. Dev.* **88**, 123–126 (1999).[Article](#) [CAS](#) [PubMed](#) [Google Scholar](#)
- 43) Takatori, N. et al. T-box genes in the ascidian *Ciona intestinalis*: Characterization of cDNAs and spatial expression. *Dev. Dyn.* **230**, 743–753 (2004).[Article](#) [CAS](#) [PubMed](#) [Google Scholar](#)
- 44) Jose-Edwards, D. S., Oda-Ishii, I., Nibu, Y. & Di Gregorio, A. Tbx2/3 is an essential mediator within the Brachyury gene network during *Ciona* notochord development. *Development* **140**, 2422–2433 (2013).[Article](#) [CAS](#) [PubMed](#) [PubMed Central](#) [Google Scholar](#)
- 45) Joyce Tang, W., Chen, J. S. & Zeller, R. W. Transcriptional regulation of the peripheral nervous system in *Ciona intestinalis*. *Dev. Biol.* **378**, 183–193 (2013).[Article](#) [CAS](#) [PubMed](#) [Google Scholar](#)
- 46) Pasini, A., Manenti, R., Rothbacher, U. & Lemaire, P. Antagonizing retinoic acid and FGF/MAPK pathways control posterior body patterning in the invertebrate chordate *Ciona intestinalis*. *PLoS ONE* **7**, e46193 (2012).[Article](#) [ADS](#) [CAS](#) [PubMed](#) [PubMed Central](#) [Google Scholar](#)
- 47) Paxton, C., Zhao, H. H., Chin, Y., Langner, K. & Reecy, J. Murine Tbx2 contains domains that activate and repress gene transcription. *Gene* **283**, 117–124 (2002).[Article](#) [CAS](#) [PubMed](#) [Google Scholar](#)
- 48) Lu, R., Yang, A. & Jin, Y. Dual functions of T-box 3 (Tbx3) in the control of self-renewal and extraembryonic endoderm differentiation in mouse embryonic stem cells. *J. Biol. Chem.* **286**, 8425–8436 (2011).[Article](#) [CAS](#) [PubMed](#) [Google Scholar](#)
- 49) Wicht, H. & Lacalli, T. C. The nervous system of amphioxus: structure, development, and evolutionary significance. *Can. J. Zool.* **83**, 122–150 (2005).[Article](#) [Google Scholar](#)
- 50) Rossi, C. C., Kaji, T. & Artinger, K. B. Transcriptional control of Rohon-Beard sensory neuron development at the neural plate border. *Dev. Dyn.* **238**, 931–943 (2009).[Article](#) [CAS](#) [PubMed](#) [PubMed Central](#) [Google Scholar](#)

- 51) Sauka-Spengler, T. & Bronner-Fraser, M. A gene regulatory network orchestrates neural crest formation. *Nat. Rev. Mol. Cell Biol.* **9**, 557–568 (2008). [Article](#) [CAS](#) [PubMed](#) [Google Scholar](#)
- 52) Tribulo, C., Aybar, M. J., Nguyen, V. H., Mullins, M. C. & Mayor, R. Regulation of Msx genes by a Bmp gradient is essential for neural crest specification. *Development* **130**, 6441–6452 (2003). [Article](#) [CAS](#) [PubMed](#) [Google Scholar](#)
- 53) Suzuki, A., Ueno, N. & Hemmati-Brivanlou, A. *Xenopus* msx1 mediates epidermal induction and neural inhibition by BMP4. *Development* **124**, 3037–3044 (1997). [CAS](#) [PubMed](#) [Google Scholar](#)
- 54) Satou, Y., Kawashima, T., Shoguchi, E., Nakayama, A. & Satoh, N. An integrated database of the ascidian, *Ciona intestinalis*: Towards functional genomics. *Zoolog. Sci.* **22**, 837–843 (2005). [Article](#) [CAS](#) [PubMed](#) [Google Scholar](#)
- 55) Anders, S. & Huber, W. Differential expression analysis for sequence count data. *Genome. Biol.* **11**, R106 (2010). [Article](#) [CAS](#) [PubMed](#) [PubMed Central](#) [Google Scholar](#)
- 56) Satou, Y., Imai, K. & Satoh, N. Action of morpholinos in *Ciona* embryos. *Genesis* **30**, 103–106 (2001). [Article](#)
- 57) Fransen, M.F.J. et al. (2021). Bioprinting of kidney in vitro models. *Essays Biochem.* <https://portlandpress.com/essaysbiochem/article/65/3/587/918458>
- 58) Ozbolat, I.T. et al. (2016). Bioprinting toward organ fabrication: challenges and future trends. *IEEE Trans Biomed Eng.* <https://ieeexplore.ieee.org/document/7457231>
- 59) Gudapati, H. et al. (2016). Inkjet bioprinting—A versatile tool for tissue engineering. *Biotechnol Bioeng.* <https://doi.org/10.1002/bit.25997>
- 60) Zhu, W. et al. (2017). 3D printing of organs-on-chips. *Biomaterials.* <https://doi.org/10.1016/j.biomaterials.2017.01.005>
- 61) Lam, E.H.Y. et al. (2023). 3D bioprinting for next-generation personalized medicine. *Int J Mol Sci.* <https://www.mdpi.com/1422-0067/24/7/6357>
- 62) Kim, Y.K. et al. (2019). Patient-specific iPSC-derived organoids for drug screening. *Stem Cell Reports.* [https://www.cell.com/stem-cell-reports/pdf/S2213-6711\(19\)30450-0.pdf](https://www.cell.com/stem-cell-reports/pdf/S2213-6711(19)30450-0.pdf)
- 63) Kim, B.S. et al. (2015). Biomaterials for 3D bioprinting. *Biotechnol J.* <https://doi.org/10.1002/biot.201400671>
- 64) Jang, J. et al. (2019). 3D printed complex tissue construct using decellularized ECM. *Nat Commun.* <https://www.nature.com/articles/s41467-019-09652-x>
- 65) Homan, K.A. et al. (2016). Bioprinted kidney proximal tubule models. *Nat Biomed Eng.* <https://www.nature.com/articles/s41551-016-0005>
- 66) Skylar-Scott, M.A. et al. (2019). Vascular network bioprinting. *Science.* <https://www.science.org/doi/10.1126/science.aav9750>
- 67) Garreta, E. et al. (2021). Tissue engineering and regenerative medicine for kidneys. *Nat Rev Nephrol.* <https://www.nature.com/articles/s41581-021-00462-3>
- 68) Murphy, S.V., Atala, A. (2014). 3D bioprinting of tissues and organs. *Nat Biotechnol.* <https://www.nature.com/articles/nbt.2958>
- 69) [1] Jager, K. J., Kovesdy, C., Langham, R., Rosenberg, M., Jha, V., & Zoccali, C. (2019). A single number for advocacy and communication-worldwide more than 850 million individuals have kidney diseases. *Kidney International*, 96(5), 1048–1050. <https://doi.org/10.1016/j.kint.2019.07.012>
- 70) [2] Wang, Y., et al. (2022). Kidney regeneration and organoids for disease modeling. *Cell Stem Cell*, 29(7), 965–979. <https://doi.org/10.1016/j.stem.2022.06.001>
- 71) [3] Morizane, R., & Bonventre, J. V. (2017). Generation of nephron progenitor cells and kidney organoids from human pluripotent stem cells. *Nature Protocols*, 12, 195–207. <https://doi.org/10.1038/nprot.2016.154>
- 72) [4] Homan, K. A., et al. (2019). Flow-enhanced vascularization and maturation of kidney organoids in vitro. *Nature Methods*, 16(3), 255–262. <https://doi.org/10.1038/s41592-019-0325-y>
- 73) Takasato, M., et al. (2015). Kidney organoids from human iPS cells. *Nature*, 526, 564–568. <https://www.nature.com/articles/nature15695>

- 74) [6] Freedman, B. S., et al. (2015). Modelling kidney disease with CRISPR-mutant kidney organoids derived from human pluripotent epiblast spheroids. *Nature Communications*, 6, 8715. <https://doi.org/10.1038/ncomms9715>
- 75) [7] Lawlor, K. T., & Little, M. H. (2021). Kidney organoids: A translational journey. *Trends in Molecular Medicine*, 27(9), 813–822. <https://doi.org/10.1016/j.molmed.2021.05.002>
- 76) [8] Schumacher, A., et al. (2020). Bioprinting of 3D kidney tissue. *Advanced Healthcare Materials*, 9(18), 2000737. <https://doi.org/10.1002/adhm.202000737>
- 77) [9] Low, L. A., et al. (2021). Organs-on-chips: Into the next decade. *Nature Reviews Drug Discovery*, 20, 345–361. <https://doi.org/10.1038/s41573-020-0079-3>
- 78) [10] Czerniecki, S. M., et al. (2018). High-throughput screening enhances kidney organoid differentiation. *Nature Methods*, 15(11), 955–962. <https://doi.org/10.1038/s41592-018-0189-y>
- 79) [11] Forbes, T. A., et al. (2018). Patient-iPSC-derived kidney organoids show functional disease phenotypes. *Nature Communications*, 9, 5389. <https://doi.org/10.1038/s41467-018-07874-9>
- 80) [12] Musah, S., et al. (2017). Mature podocytes derived from human pluripotent stem cells. *Nature Biomedical Engineering*, 1(9), 1–12. <https://doi.org/10.1038/s41551-017-0130-0>
- 81) [13] Nishinakamura, R. (2019). Human kidney organoids: Progress and remaining challenges. *Nature Reviews Nephrology*, 15, 613–624. <https://doi.org/10.1038/s41581-019-0165-x>
- 82) [14] van den Berg, C. W., et al. (2018). Renal subcapsular transplantation of PSC-derived kidney organoids induces neo-vasculogenesis and significant glomerular and tubular maturation in vivo. *Stem Cell Reports*, 10(3), 751–765. <https://doi.org/10.1016/j.stemcr.2018.01.041>
- 83) [15] Lavazza, A., & Farina, M. (2020). Stem cell-derived embryo models and chimeras: Ethical issues. *Stem Cell Reports*, 14(6), 1046–1055. <https://doi.org/10.1016/j.stemcr.2020.05.001>
- 84) [16] Kim, Y. K., et al. (2021). Gene editing and kidney organoids for modeling and therapy. *Nature Reviews Nephrology*, 17(10), 655–667. <https://doi.org/10.1038/s41581-021-00441-9>
- 85) [17] Shuaib, M., et al. (2023). Blockchain in regenerative healthcare: Traceability of bioengineered organs. *Journal of Biomedical Informatics*, 136, 104352. <https://doi.org/10.1016/j.jbi.2022.104352>